# Hygric properties of wheat straw biocomposite containing natural additives intended for thermal insulation of buildings

Naïma Belayachi, Brahim Ismail, Dashnor Hoxha

# Hygric properties of wheat straw biocomposite containing natural additives intended for thermal insulation of buildings

Brahim ISMAIL[1], Naima BELAYACHI[1], Dashnor HOXHA[1]

[1] Université d'Orléans, INSA Centre Val de Loire, Université de Tours, Laboratoire de Mécanique Gabriel Lamé Polytech Orléans, 8 rue Léonard de Vinci, 45072 Orléans, France

Corresponding author:

**Brahim ISMAIL**

Tel : 330238492502

Fax : 330238417063

Email-address: brahim.ismail@univ-orleans.fr

Postal address : Laboratoire de Mécanique Gabriel Lamé Polytech Orléans

8 Rue Léonard De Vinci

45072, Orléans cedex 2, France

## Highlights

- The hygroscopic properties of wheat straw external insulation materials are assessed.
- The isothermal water vapour diffusivity was estimated from the sorption curve and the water vapor permeability.
- The impact of material's thickness on moisture buffer value was studied

## Abstract

Straw concrete is a biobased composite developed for thermal insulation of new buildings and thermal rehabilitation of old buildings. It is made of the combination of wheat straw, lime

or plaster binder and natural additives (hemoglobin, casein, gelatin). The natural additives are used to improve the thermal and mechanical properties of the material. The characterization of these composites has shown an attractive thermal conductivity and an acceptable mechanical strength. The present paper focuses on the hygric characterization of these materials which have different constituents (straw aggregates, binder and additives). Three properties were experimentally determined, namely, sorption-desorption curves, water vapor permeability and moisture buffer value (MBV). These hygroscopic properties are of great importance when it comes to the comfort of the building. The isothermal water vapour diffusivity was also estimated from the sorption curve and the water vapor permeability. The impact of the sample thickness on the moisture buffer value (MBV) was also highlighted. The results showed that the studied composites have excellent hygric properties which can contribute significantly to ensure hygrothermal comfort in buildings. These hygric performances are competitive with those of other insulating bio-based materials studied in the literature and better than those of conventional materials used in construction.

**Keywords**: Wheat straw, lime, gypsume, sorption-desorption, water vapor permeability, moisture buffer value.

# 1 Introduction

The use of porous biobased insulators in the construction of new buildings or the rehabilitation of old ones offers many advantages such as biodegradability, renewability, local abundance, and carbon dioxide storage, which contribute significantly to improving the energy efficiency of the building and compliance with environmental requirements [1–3].

The hygric behavior of porous materials is generally studied through three properties: sorption-desorption isotherms, permeability to water vapor and the moisture buffer value [4–6]. The sorption-desorption curves are essential to evaluate the modifications of the properties

caused by the hygroscopic behavior and to deduce the water vapor diffusion properties. In general, due to their high hygroscopicity as most of the porous materials, the sorption isotherms of the materials based on vegetable aggregates present a sigmoidal form of type II or III according to the IUPAC classification [7]. Biobased composites have a high moisture storage capability compared to other building materials. Samri 2008 [8] compared the adsorption isotherms of three materials, namely aerated concrete clay and hemp concrete. He noticed that the moisture storage capacity of the hemp concrete is higher when the relative humidity is between 40% and 90% unlike the other two materials. According to the author, this property (moisture storage capacity) has a direct consequence on the capacity of the materials to fluctuations in relative humidity, present the room (human activity, kitchen, bathroom). The different vegetal concretes studied in the literature show a similar behaviour. For the adsorption isotherm, the mass water content of the materials increases progressively as a function of relative humidity up to 80% RH depending on the constituents of each composite. Beyond RH=80% the water content increases rapidly to reach values between 10 and 26% depending on the material [8–11]. Conversely, in desorption, the water content decreases rapidly from RH=98% to RH=80% and then evolves progressively between RH=80% and low humidity [8–11]. From this very sensitive behevior to humidity, an important hysteresis between the adsorption and the desorption isotherm is present and has been highlighted by several authors for the different composites of plant-based concretes [8–11]. It has been noted that the water content of the material observed in adsorption for a given relative humidity is lower than that observed in desorption. This difference is explained by the existence of pores in the shape of ink bottle.

The effect of the type of constituents (aggregates, binders) and their fractions on the adsorption isotherm has also been discussed, Mazhoud 2017 [12] noted that composites with a lime-based matrix possess a higher water content than composites with a clay-based matrix.

However, Chamoin 2013 [13] showed that the binder type slightly impacts the adsorption-desorption isotherm of hemp concrete. Indeed, the substitution of the lime-based binder with a calcium sulfate-based binder leads to a similar water content value, except at high relative humidity (above 80% RH), where capillary condensation occurs. Belayachi et al 2015 [14], found no influence of aggregate type on the adsorption-desorption isotherms of straw concrete. Barley straw-based composites have similar curves to that of wheat straw-based composites. Brouard et al 2018 [15] did not observe a significant difference between the behavior of rapeseed-based formulations and those with sunflower bark. On the other hand, other authors have observed that an increase in the aggregate/binder ratio leads to higher moisture content values, especially at high relative humidities. This was attributed, on the one hand, to a higher polymolecular adsorption and on the other hand, to capillary condensation [9,12,16]

The water vapor permeability represents the capacity of a material to transfer moisture. The determination of this parameter is essential in the hygric characterization of materials and their use in the design of effective thermal insulation of buildings. The most used method in the literature to measure this coefficient is the cup method, described in the standard EN ISO 12572 [17].

Overall, due to their high open porosity, the water vapor permeability of plant-based materials is high. Several authors in the literature have studied the water vapor permeability of plant-based materials using the cup method [17]. Collet 2004 [18], Evard 2008 [19], Chamoin 2013 [13], Walker et al 2014 [20], Bennai 2017 [11] determined the water vapor permeability of the various hemp concrete mixtures. They found values between 1.6 $.10^{-11}$ and 3 $.10^{-11}$ (kg/m.s.Pa) depending on the constituents of each composite. Rahim et al 2015 [21], Rahim et al 2016 [22], obtained a value of 2 $.10^{-11}$ and 4.5 $.10^{-11}$ (kg/m.s.Pa) for rape straw concrete and a value of 2.34 $.10^{-11}$ (kg/m.s.Pa) for flax concrete. These experimental values proposed

by various authors confirm the same order of magnitude for the different biobased materials without much effect of aggregate and binder type.

The relative humidity is a factor that strongly influences the water vapor permeability. Kumaran et al 2002 [23], Collet et al 2013 [16] determined the water vapor permeability of biobased composites as a function of the humidity. They indicated that the permeability evolves according to an exponential or power law with increasing humidity.

The measurement of water vapor permeability and the determination of adsorption-desorption isotherms allow to deduce the isothermal water vapour diffusivity. This coefficient characterizes the change rate of the water content of a material under transient changes in humidity. Collet et al 2012 [24], Rahim et al 2015 [21] and Rahim et al 2016 [22] estimated the water vapour diffusivity coefficient for hemp, rapeseed and flax concrete, they found values between $10^{-10}$ and $10^{-7}$ $m^2/s$.

Among the hygric parameters of porous materials of interest for the design of a comfortable indoor environment, the Moisture Buffer Value (MBV). This property indicates the ability of the material to regulate the moisture variations in the ambient air. The MBV is measured according to the approach defined in the Nordtest Project Rode et al. 2005 [25]. According to several works in the literature [10,21,22,24,26–29] plant-based concretes have shown a MBV higher than $2g/(m^2.\%RH)$, which allowed them to be classified as an excellent water regulators according to the classification of Rode et al 2005 [25].

The present paper aims to study the hygric behavior of three biobased materials, developed in the framework of the research program PEPITE with a great potential of thermal insulation of buildings by interior or exterior [30]. These new materials are based on cereal straw, lime or gypsum binder and additives from a renewable and biodegradable source to optimize their performances for the hygrothermal comfort of buildings. Three hygric

properties were experimentally determined, namely sorption-desorption curves, water vapor permeability and moisture buffer value. The objective is to compare the hygric performance of the three optimized composites which have different constituents such as the straw fraction, the type of binder and the type of additives. The isothermal water vapour diffusivity was estimated from the sorption-desorption curves and the water buffer value. The impact of the thickness of the material on the moisture buffer value was also investigated. The influence of additives and thickness on hygric properties is analyzed based on the comparison between our research outcomes and literature findings.

# 2 Materials and methods

## 2.1 Materials

### *2.1.1 Raw materials*

- *Wheat straw:* the straw used in this study to prepare the biocomposites was harvested in the Region Centre Val de Loire in France. It was manually cut in the laboratory only in the longitudinal direction in order to maintain its natural tubular shape. The size obtained after cutting is the one that was intended for mixing with 90 % straw of 3.5 cm.

Two mineral binders were used in the present study to prepare the biocomposites:

- *Tradical PF70*: is a pre-formulated binder manufactured in accordance with the requirements of NF 459. It is based on aerial lime (75%), hydraulic binders (15%) and pozzolan (10%).
- A commercial plaster produced by Diall, wich is characterized by its quick setting time (10-15 minutes).

Three natural additives was adopted to optimize the thermal and mechanical properties of biocomposites :

- *Hemoglobin*: this is a proteinaceous substance from pork blood obtained by fractionation and spray drying. Vepro 95 PHF is the commercial name of the product used in this study and is manufactured by the Vapran Group in powder form.
- *Casein*: this is a protein extracted from milk, produced by EPI Ingredients Group in the form of a fine white powder (<400µm). It is used as a natural fixative for lime coating.
- *Gelatin*: this is a technical gelatin 200 bloom produced by the Weishardt Group in powder form with a particle size less than 20 mesh (841 µm).

### *2.1.2 Biocomposites*

Three straw composites were selected from previous work [30] for this investigation, the first one is based on lime, hemoglobin, and casein (Fig.1-a). These additives were used to increase the porosity of the matrix and improve the fiber-matrix interface. The second one is based on lime and gelatin (Fig.1-b). The last one is based on gypsum plaster and gelatin. The use of this biopolymer allows increasing of straw fraction (Fig.1-c). The manufacturing procedure of the developed biocomposite is detailed in the previous work of Ismail et al. 2020 [30]. The composites are denoted respectively LHC, LGB and GGB, as indicated in Tab. 1. The porosity of composites was determined by the pycnometer method, the values obtained for the three materials are remarkably close.

| Mixture-ID | | Mass ratio (kg/kg) | | | | Density ($Kg/m^3$) | Total porosity (%) |
|---|---|---|---|---|---|---|---|
| Short Ref | Long Ref | S/B | H/B | C/B | GB/B | | |
| LHC | Lime+5% H+2.5% C | 0.3 | 0.05 | 0.03 | - | 308 | 85.47 |
| LGB | Lime+20%GB | 0.4 | - | - | 0.2 | 288 | 85.37 |
| GGB | Gepsume+10%GB | 0.4 | - | - | 0.1 | 277 | 87.14 |

S/B: Straw/Binder H/B: Hemoglobine/Binder C/B: Caseine/Binder
GB/B: GelatinBinder/Binder.

**Tab. 1.** Composites designation and detailed mixture proportions

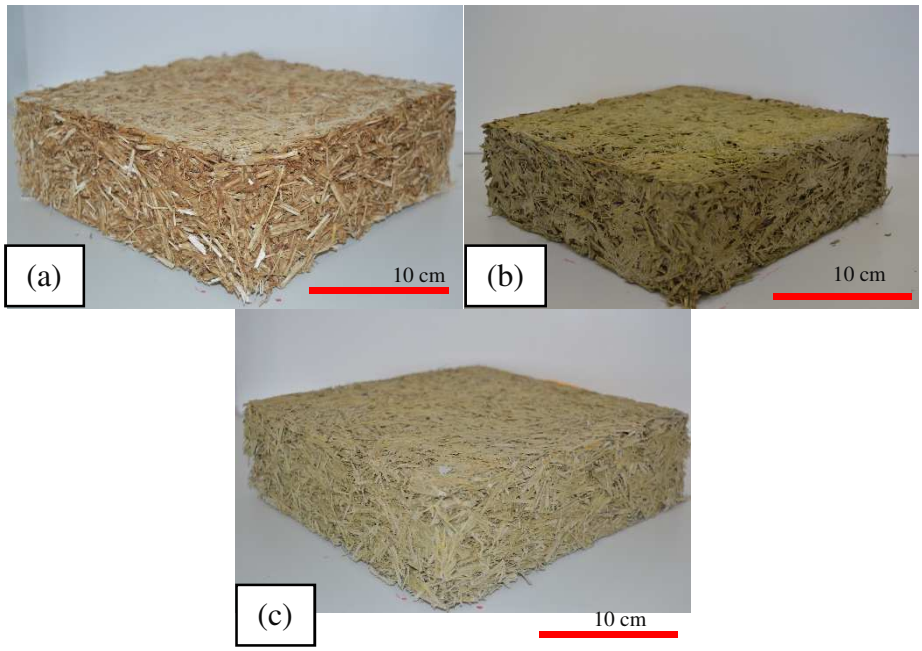


**Fig. 1**. Appearance of composites (a) LHC (b) LGB and (c) GGB

## 2.2 Methods

In order to evaluate the hygric behavior of the selected biocomposites, three types of experimental tests were carried out, the sorption-desorption, the water vapor permeability and the moisture buffer value

### *2.2.1 Sorption-desorption isotherms*

Sorption-desorption isotherms are often determined by gravimetric measurement, where material samples are placed in different relative humidities at constant temperature. Mass tracking is used to determine the equilibrium point and to calculate the water content for a given humidity. The most commonly used method is the saline solution method, which allows the use of nine humidity levels between 10% and 98%.

In this work, the sorption-desorption curves of the three composites were determined automatically using Vsorp equipment from ProUmid GmBH, (Fig. 2). The device is equipped with a sample tray and a balance with a resolution of 100 µg. The sample tray is located in a

climatic chamber with controlled temperature and humidity. Materials samples of approximately 5 × 5 × 5 $cm^3$ were prepared for each composite and dried at 60°C until constant mass was reached. Then, the material samples were placed in aluminium pans of sample tray. Nine humidity levels (varying from 10% to 90% RH with a 10% step) were set at a constant temperature of 25°C. The weighing of the samples was performed automatically every 15 min. Equilibrium is assumed to be reached when the mass variation does not exceed 0.01% within 24 h.

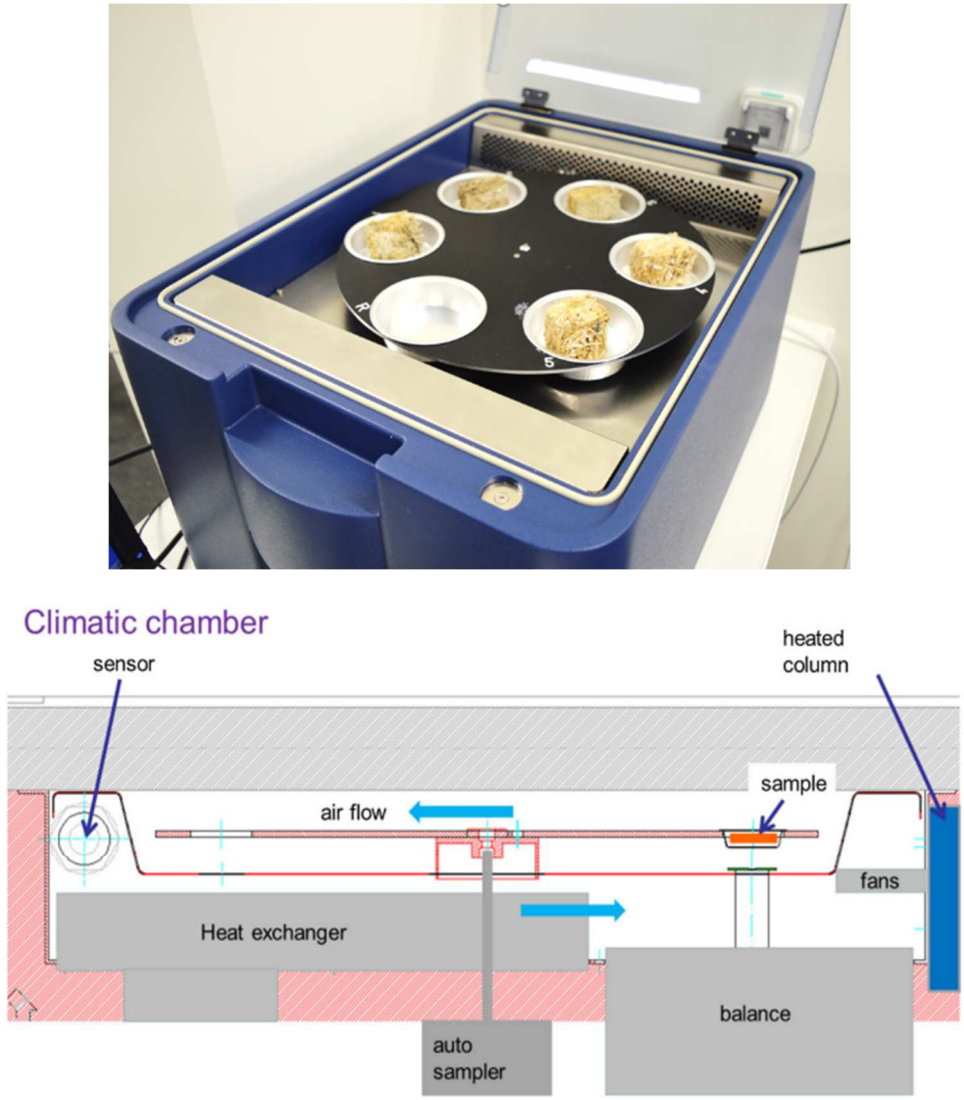


**Fig. 2**. Sorption-desorption test (Vsorp equipment)

### 2.2.2 *Water vapour permeability*

The Vsorp equipment was also used here to measure the water vapor permeability of the composites based on the cup method according to the European Standard EN ISO 12572 [10]. The test procedure consists of applying a pressure difference between the upstream and downstream sides of the specimen and then calculate the amount of water vapor flow through the material (Fig. 4). The density of water vapor flow rate, g, is given by the following equation:

$$g = \frac{G}{A} \tag{1}$$

With :

A : is the exposed area of the test specimen ($m^2$)

G: represents the mass change rate, calculated from the mass versus time curve. According to the standard EN ISO 12572 [10], the value of G is obtained when each of the last five successive determinations of $\Delta m_{12}$ is within ±5% of G (the mean of five successive determinations).

Where :

$$\Delta_{12} = \frac{m_{i+1} - m_i}{t_{i+1} - t_i} \tag{2}$$

With : $m_i$ is the mass at time $t_i$; $m_{i+1}$ is the mass at time $t_{i+1}$

The moisture transfer under a vapour pressure gradient can be expressed as:

$$g = -\delta \nabla p_v \tag{3}$$

So, the water vapour permeability, δ (kg/(m.s.Pa)), is given by the equation 3 :

$$\delta = g \frac{e}{\Delta p_v} \tag{4}$$

Where :

e : is the thickness of the test specimen in m

Δp : is the water vapour pressure difference Pa

The vapour pressure on either side of the specimen was calculated from the temperature (T) and relative humidity (HR) according to the formula proposed by the standard [10]:

$$p_v = \mathrm{HR}.\,610.5\ \mathrm{e}^{\frac{17.269\,\mathrm{T}}{237.3+\mathrm{T}}} \quad (5)$$

In order to take into account, the resistances of the layer of air in the test cup between the base of the specimen and the desiccant or saturated salt solution, and on both internal and external sides of the specimen. The standard EN ISO 12572 [10] and other works [20-21] of the literature proposes to correct the water vapour permeability calculated in formula 2 by formula:

$$\delta = \frac{e}{\frac{\Delta pv}{g} - (Z_{p,air} + Z_{p,in} + Z_{p,out})} \quad (6)$$

With :

$Z_{p,air}$: is the resistances of the layer of air in the test cup between the base of the specimen and the desiccant or saturated salt solution is given by:

$$Z_{p,air} = \frac{d_a}{\delta_a} \quad (7)$$

Where $d_a$ (1.5 cm) is the thickness of the air layer and $\delta_a$ is the water vapour permeability of air.

$Z_{p,in}$ and $Z_{p,out}$ ((Pa.m$^2$ s)/kg) are the resistance of the boundary layers which can be estimated from the convective mass transfer coefficients ( $_p$) [20-21].

$$Z_p = \frac{1}{\beta_p} \quad (8)$$

231 $_p$ is estimated using the following equation:

$$\frac{1}{\beta_p} = \frac{R_v . T . (\rho . Cp)_{air}}{h_c} \, Le^{3/4} \quad (9)$$

232 where q is the air density (125 kg/m$^3$), Cp: heat capacity of air (1005 J/(kgK)), Rv: gas
233 constant for vapor (461.5 (J/(kgK)), T: temperature (20°C), Le is the Lewis number (ratio
234 between the thermal diffusivity to vapor diffusivity of air and the volumetric heat capacity of
235 air), and hc: the convective heat transfer coefficient (W/(m$^2$K)), is estimated from the air
236 velocity (m/s) by the following relation [20-21]:

$$hc = 5.83 + 3.96. \quad (10)$$

237 The $h_{c,out}$ is calculated from the air velocity above the specimen (0.25 m/s) and $h_{c,in}$ is
238 calculated from the air velocity below the specimen (0 m/s).

239 Several works in the literature also use the vapor resistance factor ( ) instead of the water
240 vapor permeability:

$$\mu = \frac{\delta_a}{\delta} \quad (11)$$

241 where $\delta_a$ is the water vapor permeability of air (2.10$^{-10}$kg/(m.s.Pa)).

242 In this work, the water vapor permeability of composites was evaluated under dry cup
243 (3%/50% RH) and wet cup (93%/50% RH) conditions. The tests were performed at 23°C, the
244 50% RH was provided with a climatic chamber of Vsorp equipment and the 3% RH or 93%
245 RH was maintained by the molecular sieve (spherical metal aluminium silicates with sphere

diameters between 1.6 and 2.5 mm) and the saturated salt solutions of $KNO_3$, respectively. Circular samples with a diameter of 8.5 cm and a thickness of about 1 cm, were prepared in cylindrical cardboard moulds for each material (Fig. 3). After a curing period of 28 days, the specimens were conditioned at 50% RH and 20°C until mass stabilization. To avoid errors due to leakage, a mixture of 60% of microcrystalline wax with 40% refined crystalline paraffin was used to ensure a seal between the sample and the cup. The weighing of the cups is programmed every 10 minutes.

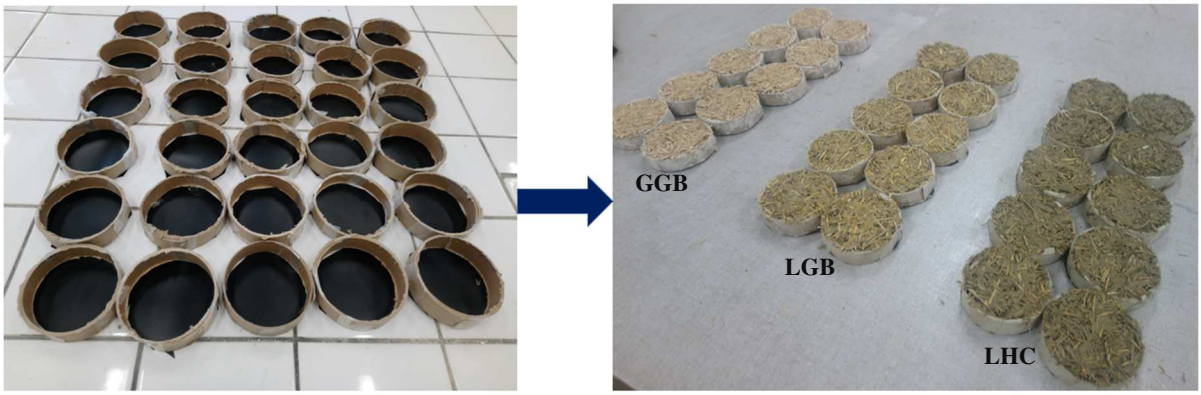


**Fig. 3** : Preparation of samples for water vapor permeability test (a) cylindrical cardboard moulds (b) samples of composites

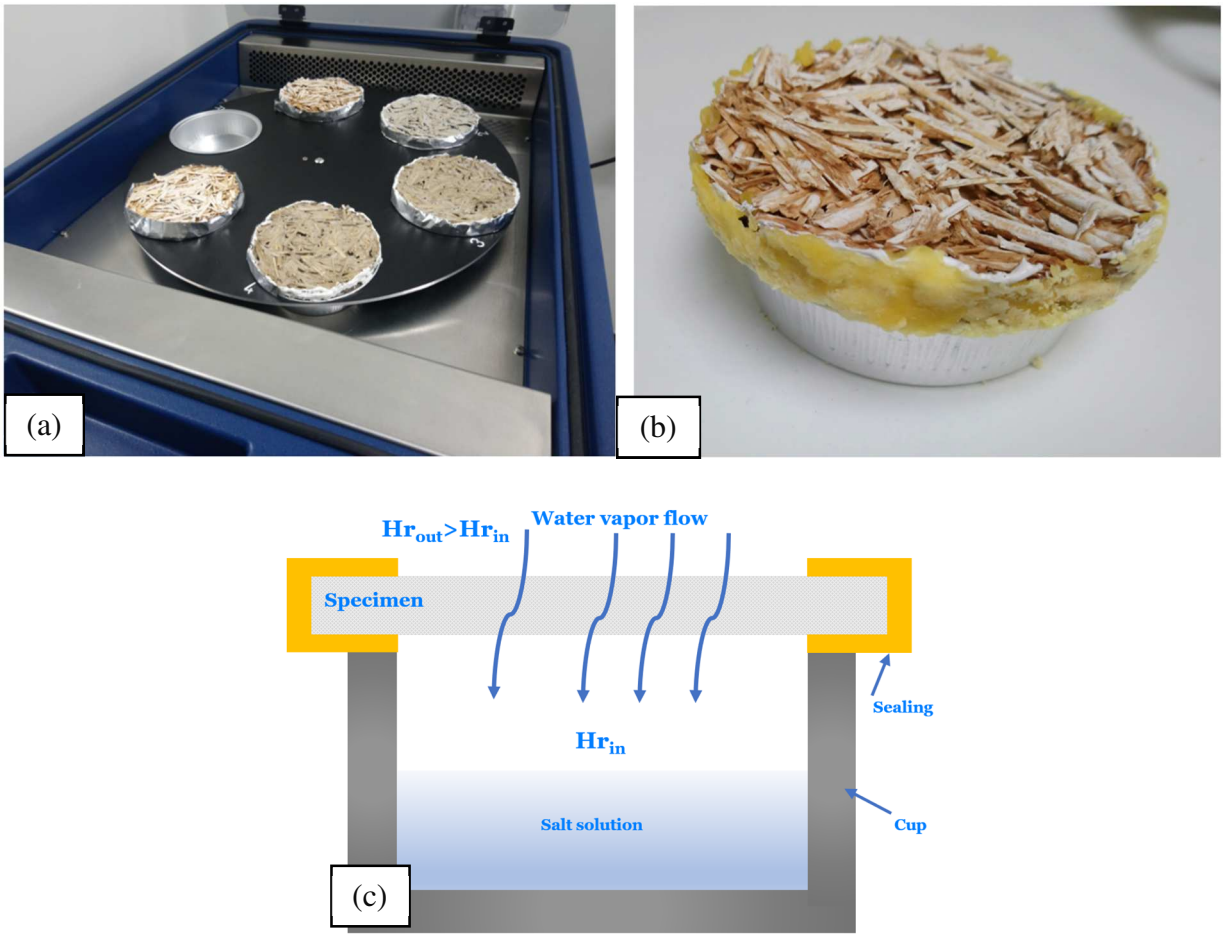


**Fig. 4**. Water vapor permeability test (a) experimental device (Vsorp) (b) and (c) sample+cup used for measuring water vapor permeability according to standard cup-method

### *2.2.3 Isothermal water vapour diffusivity*

The combination of the results obtained for the adsorption isotherms and the water vapor permeability allows the calculation of the isothermal water vapour diffusivity Dw. Indeed, under isothermal conditions, the vapour flux density is given by the following equation:

$$g = -D_w \nabla \omega \qquad (12)$$

With :

$D_w$: water vapour diffusivity in m $^2$/s

ω: water content in kg/m$^3$

For a one-dimensional transfer the equation can be written as a function of the relative humidity as follows :

$$g = -D_w p_{sat} \frac{\partial HR}{\partial x} \quad (13)$$

HR : relative humidity

$p_{sat}$: saturated vapor pressure in Pa

So, the isothermal water vapour diffusivity is calculated from sorption and water vapour permeability according to the following equation:

$$D_w = \frac{p_{sat}.\delta}{\frac{\partial \omega}{\partial HR}} \quad (14)$$

$\frac{\partial \omega}{\partial HR}$ represents the derivative of the adsorption isotherm which reflects the moisture storage capacity of the material.

In order to calculate $\frac{\partial \omega}{\partial HR}$, a modeling of the adsorption isotherm is necessary. For that, several models were used in the literature, such as the model of Langmuir 1918 [31], the model of Brunauer-Emmet-Teller (BET) [32], the model of Guggenheim-Anderson- DeBoer (GAB) or the model of Generalised-D'Arcy-Watt (GDW). These last two are derivatives of the Langmuir model and are the most widely used in the literature.

In this study, the GAB model was used to smooth the adsorption curve of the three composites. The expression of this model is given by the following equation:

$$\omega = \frac{\omega_m C_2 C_3 HR}{(1 - C_3 HR)(1 - C_3\, HR + C_2 C_3 HR)}$$

$$C_2 = \exp\left(\frac{E_l - E_m}{RT}\right), C_3 = \exp\left(\frac{E_L - E_m}{RT}\right)$$

289 With :

290 w : water content by mass of the material,

291 $w_m$ : water content of the material when the walls are completely covered,

292 $E_l$ : molar heat of adsorption in J/mol,

293 $E_L$ : latent molar heat of vaporization in J/mol,

294 T : temperature in K,

295 R : perfect gas constant.

296 The constants $\omega_m$, $C_2$ and $C_3$ are determined by fitting the GAB model to the experimental

297 measurements using the least squares method.

298 *2.2.4 Moisture buffer value (MBV)*

299 The moisture buffer value is measured according to the protocol developed by Rode et al

300 2005 [25]. The test was performed using a Binder climatic chamber. The samples were

301 subjected to a cycle of 24 hours in which the relative humidity was fixed at 75% for 8 hours

302 and then at 33% for 16 hours (Fig. 5). An adjustment of the chamber fan speed was necessary

303 to obtain the value recommended by the protocol (0.1 ± 0.05 m/s) in the vicinity of the

304 samples. The samples were weighed five times in the adsorption phase and twice in the

305 desorption phase using a balance with a resolution of 0.01 g. The test was stopped when the

306 difference between the mass variations recorded became less than 5% over the last three

307 cycles. The moisture buffer value was calculated according to the following equation:

$$MBV = \frac{\Delta m}{A.\left(HR_{\text{High}} - HR_{Low}\right)} \quad (15)$$

308 Where :

309 MBV: is the moisture buffer value (g/m$^2$.RH (%)),

310 Δm : is the mass variation during the sorption or desorption phase (g),

311 A : is the exchange surface (m$^2$),

312 $HR_{High}$, $HR_{Low}$ : are (75 %) for the high relative humidity and and (33 %) for the lower one.

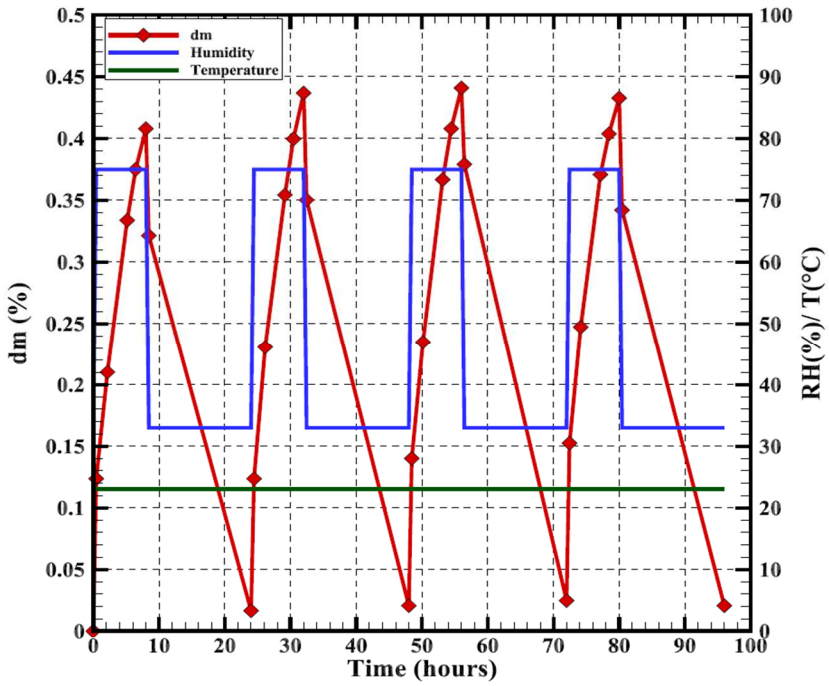


313

314 **Fig. 5**. Example of a moisture uptake and release cycles for a sample

315 In order to evaluate the influence of material thickness on MBV, four thicknesses were
316 studied for each composite: 6 cm, 8 cm, 10 cm and 12 cm. Three samples with an area of 10 ×
317 10 $cm^2$ were prepared for each composite and each thickness (Fig. 6). All sample surfaces are
318 protected with adhesive aluminium tape to leave a single exchange surface as shown in Fig. 7.


319

**Fig. 6** : Experimental setup and placement of samples

# 3 Results and discussion

### *3.1.1 Sorption-desorption isotherms*

Fig. 7 shows the mass variation of the three composites as a function of time for the different humidity levels imposed at constant temperature. It can see that for the humidity levels below 80% RH, the mass stability was reached in a few days. However, for the 90% humidity value, the kinetics of mass gain becomes very slow, especially for lime-based composites. The achievement of equilibrium required two months respectively for LGB and LHC compared to 4 days for the gypsum plaster-based composite (GGB). This shows that the binder type influences the moisture adsorption kinetics of the composites. It was observed that during the 90% humidity level, the water content of the plaster composite (GGB) was decreased slightly (by 1%) between 60 days and 110 days. This reduction may be due to the formation of mold in this composite which leads to the modification of its water content. Indeed, it was observed at the end of the test an appearance of mold inside and on the surface of the samples of this material. The curves also show that the desorption kinetics is very fast compared to the adsorption kinetics. The desorption path time is approximately 18 days against 4 months for adsorption path. This shows the very long time necessary for the hygric characterization of porous materials, and the biobased materials particularly.

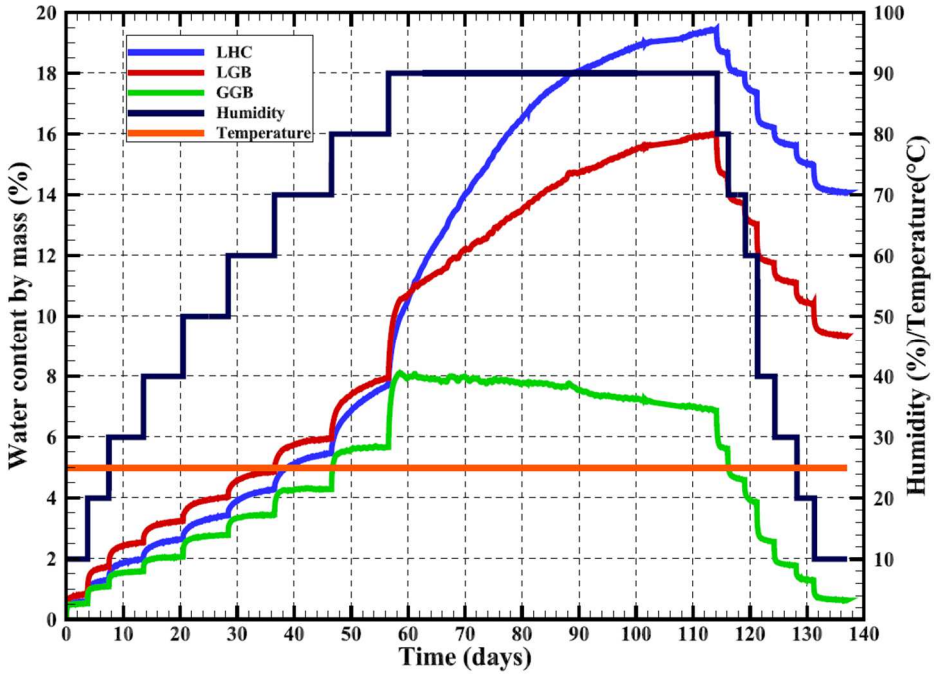


**Fig. 7.** Mass variation as a function of time at different humidity levels

Fig. 8 shows the sorption-desorption isotherms for the three studied composites. The shape of the curves is similar to that found in the literature for other plant-based materials. For the LHC and LGB lime-based composites, the water content in adsorption increases progressively and almost linearly with the increase in humidity up to a RH=80%. Beyond this last value, the water content increases rapidly to reach a value of 20% and 16% respectively for LHC and LGB. In desorption, the water content decreases progressively and linearly over the whole moisture range until reaching a value of 14% and 9.8% for a humidity of about 10 %. This was reflected in a large hysteresis that was observed over all humidity levels for lime based biocomposite. This hysteresis can be explained by the existence of the « ink bottle » shaped pores but also by the consumption of $H_2O$ during the carbonation reaction. Indeed, as it has been noted above, the samples tested had a cure time of 28 days, whereas the complete carbonation of lime can last several months [33].

For the gypsum-based composite (GGB), the increase in water content was almost linear over the whole study humidity range, a small hysteresis was observed between RH=40% and RH=70% but with a negligible area compared to that observed in the case of lime-based composites.

Fig. 9 shows a comparison of the adsorption desorption curves of the studied composites with those of other biobased materials from the literature. The evolution of the water content in adsorption and desorption is almost similar between the different materials. However, it is clear that the hysteresis between the adsorption and desorption curve of LHC and LGB composites is more significant than that of other materials in the literature. The hysteresis observed in the case of plaster-based composite (GGB) is less important than that of hemp concrete. These results can be explained by the variation of the constituents such as the binder type, the binder content, and the nature of the plant aggregates which results in a different porosity network and consequently a different hygric behaviour of the materials.

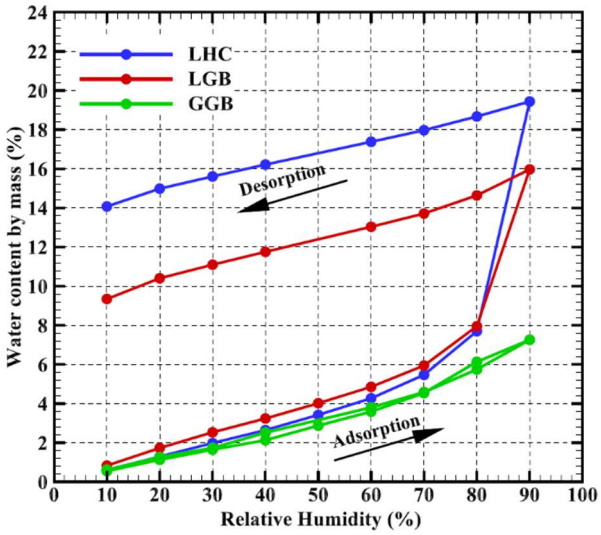


**Fig. 8.** Adsorption-desorption isotherms of the three composites

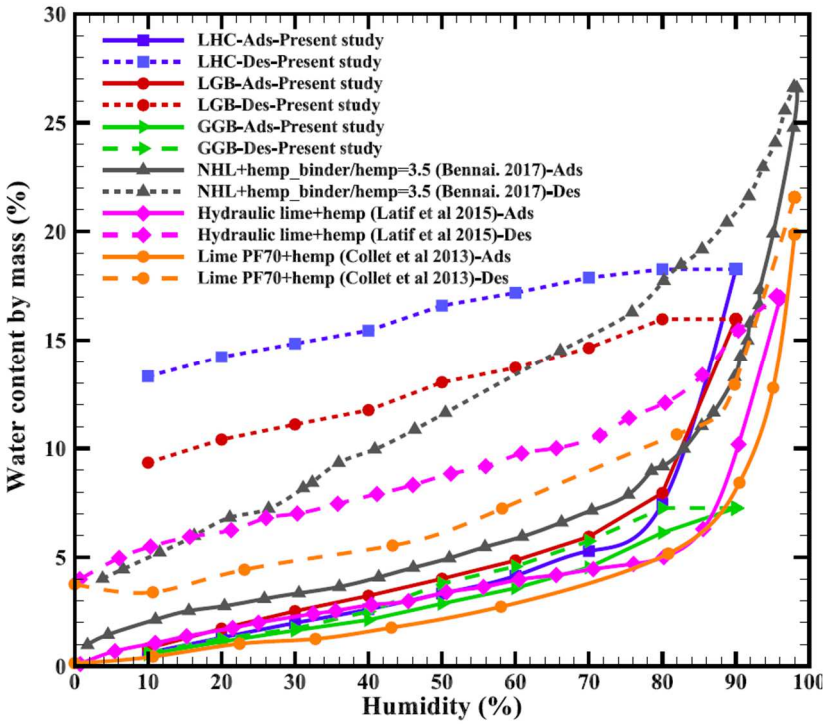


**Fig. 9.** Adsorption-desorption isotherms of the studied composites with other biobased materials in the literature

### *3.1.2 Water vapor permeability*

The mass variation (cup and sample) is illustrated in Fig. 10 as a function of time, obtained for the dry and wet cup chosen here for the study. It can be seen that the saturation of molecular sieve was reached during 24 h, because of its ability to absorb moisture very quickly. These curves were used to calculate the flow density through the samples in order to deduce the water vapor permeability.

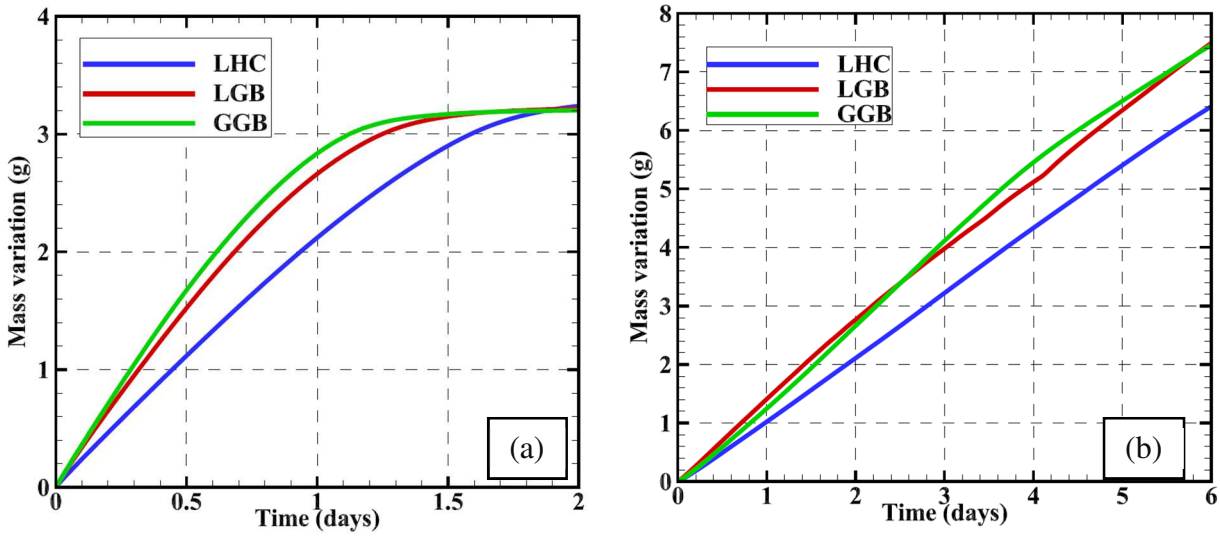


390 **Fig. 10.** Variation of mass as a function of time (a) dry cup (3%/50%) (b) wet cup (50% /
391 93%)

392 We can notice that the deduced water vapor permeability of the three composites (Fig. 11) is
393 in the same order of magnitude, both for the dry (3%/50% RH) and wet cup (50%/93% RH).
394 The values obtained in both cases are close and the standard deviation remains in the same
395 range for the three composites. This can be justified by the fact that the porosities of three
396 composites are very close (Tab. 1). We also note that the binder type has no impact on the
397 coefficient of permeability to water vapor, with values which remain quasi-similar for lime or
398 gypsum plaster in the case of the wet and dry cup. $4.3.10^{-11}$ kg/m.s.Pa. The same result was
399 showed by Chamoin 2015 [13]. They noted that the water vapor permeability remains almost
400 constant despite the substitution of a binder (Tradical PF70) by another (Microcem),
401 regardless of the replacement rate. Evard 2008 [18] also found that the water vapor
402 permeability of hemp concrete is about $4.3.10^{-11}$ kg/m.s.Pa and $4.4.10^{-11}$ kg/m.s.Pa
403 respectively for wet and dry cup.

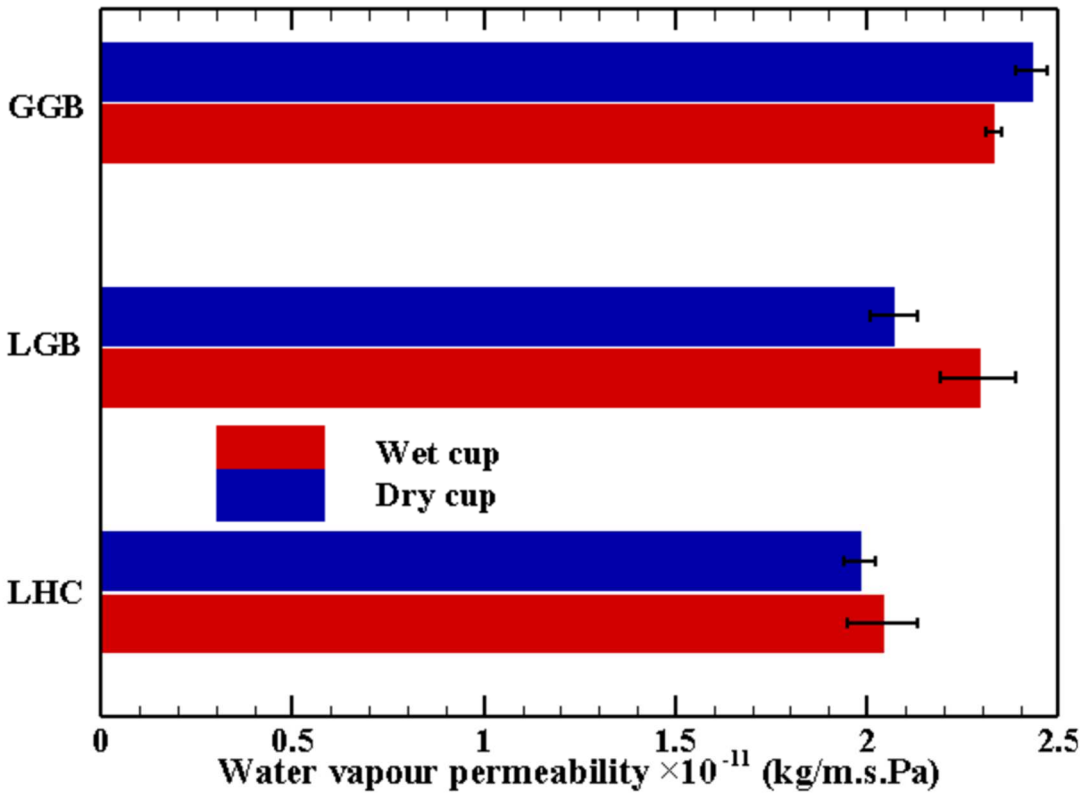


404

405 **Fig. 11**. Water vapor permeability of the three composites for the dry (3%/50% RH) and wet
406 cup (50%/93% RH)

407 The obtained values for the three composites are in the same order of magnitude as those of
408 other plant aggregate materials proposed by other authors in the literature as shown in Tab.2.
409 We compare also the vapor resistance coefficient which represents the ratio of the diffusion
410 coefficients of water vapour in air and in the building materials proposed by several studies.
411 These values show that water vapour passes quickly through the biobased materials, thus
412 avoiding the problem of condensation but it is necessary to remain vigilant in the case of
413 rehabilitation of old building and to study the composition of the existing walls.

| Material | $\rho_{app}$[kg/m$^3$] | μ[−] | References |
|---|---|---|---|
| LHC | 312 | 9.47 | Present study |
| LGB | 294 | 8.45 | Present study |
| GGB | 285 | 8.35 | Present study |
| Lime + hemp | 405 – 440 | 10 – 12 | Collet 2004 [34] |

| | | | |
|---|---|---|---|
| Lime + hemp | 400 – 466 | 5 – 7.5 | Evard 2008 [19] |
| Lime + Microcem + hemp | 406 – 475 | 6.46 | Chamoin 2013 [13] |
| Lime + treated hemp | 469 | 7.23 | Chamoin 2013 [13] |
| Lime+colza | 469 | 7.57 | Rahim et al 2016 [21] |
| Lime+flax | 469 | 8.29 | Rahim et al 2015 [20] |
| Ordinary concrete | 2300 – 2600 | 130 | R-Thermique 2005 [35] |
| Natural pumice concrete | 950 – 1150 | 50 | R-Thermique 2005 [35] |
| Autoclaved aerated concrete | 765 – 825 | 10 | R-Thermique 2005 [35] |
| Wood concrete | 450 – 650 | 15 | R-Thermique 2005 [35] |
| Terracotta | 2300 – 2400 | 16 | R-Thermique 2005 [35] |

**Tab. 2**. Vapor resistance coefficient of the studied materials in comparison with other materials in the literature (dry cup)

### *3.1.3 Isothermal moisture diffusivity*

As explained above, the calculation of moisture diffusivity requires the identification of the parameters of GAB model selected for fitting of the adsorption curve as shown in Fig. 12 by using the three curves for the studied biocomposites. Tab.3 gathers the estimated model parameters. It is clear that the GAB model perfectly reproduces the experimentally obtained adsorption isotherms for the three materials.

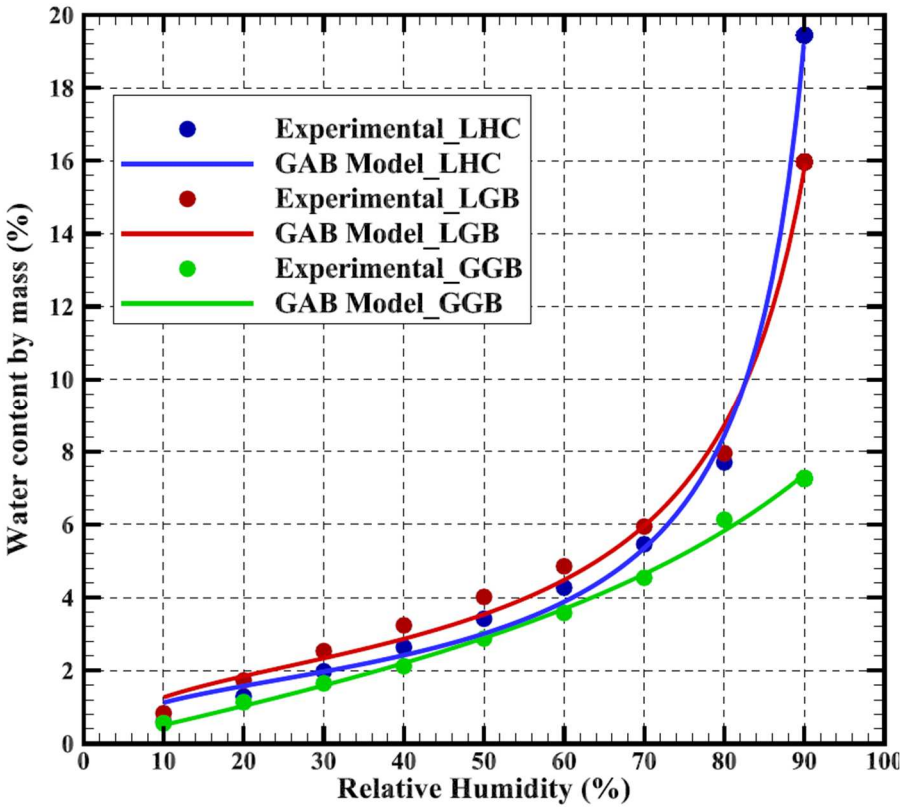


422

423 **Fig. 12**. Fitting of absorption curves using the GAB model

| Composite | $\omega_m$ (%) | $C_2$ | $C_3$ |
|---|---|---|---|
| LHC | 1.56 | 16 | 1.02 |
| LGB | 1.96 | 12.88 | 0.97 |
| GGB | 3.89 | 1.91 | 0.67 |

424 **Tab. 3** GAB model parameters

425 Finally, by introducing the storage capacity with the water vapor permeability in equation 4,
426 the evolution of the isothermal moisture diffusivity as a function of water content can be
427 deduced. The results obtained for the three composites are presented in Fig.13. We can
428 observe that the evolution of the water vapour diffusivity of two lime-based materials is
429 similar. Moreover, the shape of the three curves at low and medium water contents, coincides
430 with the one predicted by De Vries 1958 [36]. For the gypsum-based composite only the
431 decay is observed. This can be explained by the difference in the derivative of the sorption-
432 desorption isotherm curve calculated from the GAB model. On the other hand, the maximum

values of the water vapour diffusivity for the three composites are very close. They are equal to 3. 9 $10^{-9}$, 3.7 $10^{-9}$ and 3.6 $10^{-9}$ respectively for LHC, LGB and GGB. These values, as well as the evolutions of the water vapour diffusivity, obtained for the three composites are in agreement with those found in the literature for other plant-based concretes with values in the same order of magnitude ($10^{-9}$) from the works of Collet et al 2012 [24], Rahim et al 2015 [20] or Rahim et al 2016 [21].

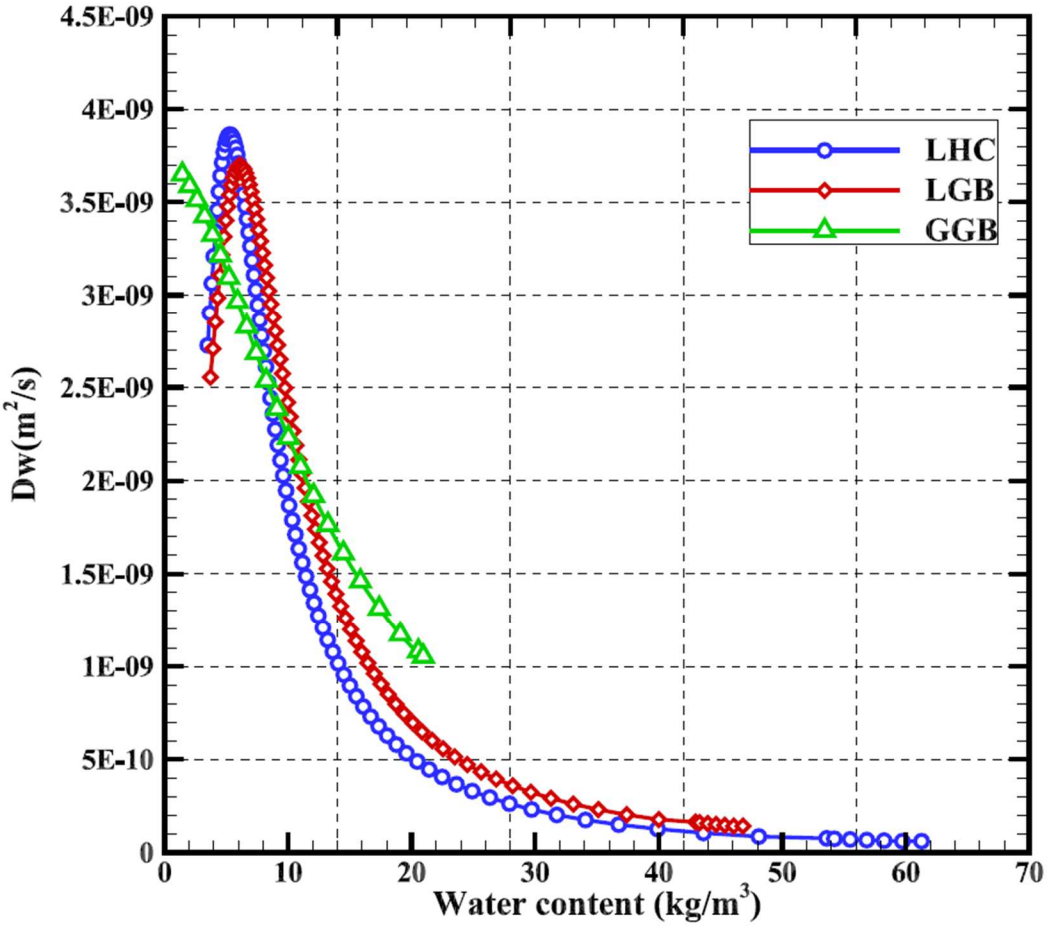


**Fig. 13**. Evolution of the isothermal water vapour diffusivity as a function of the mass water content for the three composites

### *3.1.4 Moisture buffer value (MBV)*

Fig. 14 shows the obtained moisture buffer values for the three composites and for all selected material thickness. The values represent the average of the three measurements for the three

samples used. All the values are higher than 2 (g/m$^2$ %RH) which allowed to classify the three new materials in the range of excellent moisture regulators according to the classification of Nordtest project Rode et al 2005 [25]. The values obtained for the plaster-based composite are better than those for lime-based composites. As an example, for a thickness of 12 cm, the MBV of GGB reaches a value of 3.45±0.20 (g/m$^2$ %RH) against 2.53±0.18 (g/m$^2$ %RH) and 2.66±0.12 (g/m$^2$ %RH) respectively for LGB and LHC composites. The standard deviation remains the same order of magnitude in all cases.

The evolution of the MBV with the thickness of the samples was not significant and no trend is noted. The thicknesses tested are greater than the water vapor penetration depths, which may be the reason for this result. Arfvidsson 1999 [37] defined the penetration depth ($d_{p1\%}$) of water vapor as the depth at which the amplitude of the variation of the water content is only 1% of the variation of the material surface. For a sinusoidal variation of the moisture content on the surface of the material, the penetration depth is given by the equation 6

$$d_{p1\%} = 4{,}61\sqrt{\frac{D_m t_p}{\pi}} \tag{16}$$

$D_m$ : is the water vapour diffusivity in m$^2$/s, for a relative humidity value of 54% RH (average between 33 %RH and 75% RH).

tp : is the time period in (s) (24 h in this study).

The results presented in the Tab. 4 confirm that the $d_{p1\%}$ values calculated from equation 6 are lower than the studied thicknesses.

| Composite | Dw(m$^2$/s) | $d_{p1\%(}$cm) |
|---|---|---|
| LHC | $1.78.10^{-9}$ | 3.24 |
| LGB | $1.69.10^{-9}$ | 3.15 |
| GGB | $2.38.10^{-9}$ | 3.74 |

**Tab. 4** Penetration depth (dp1%) calculated for the three composites

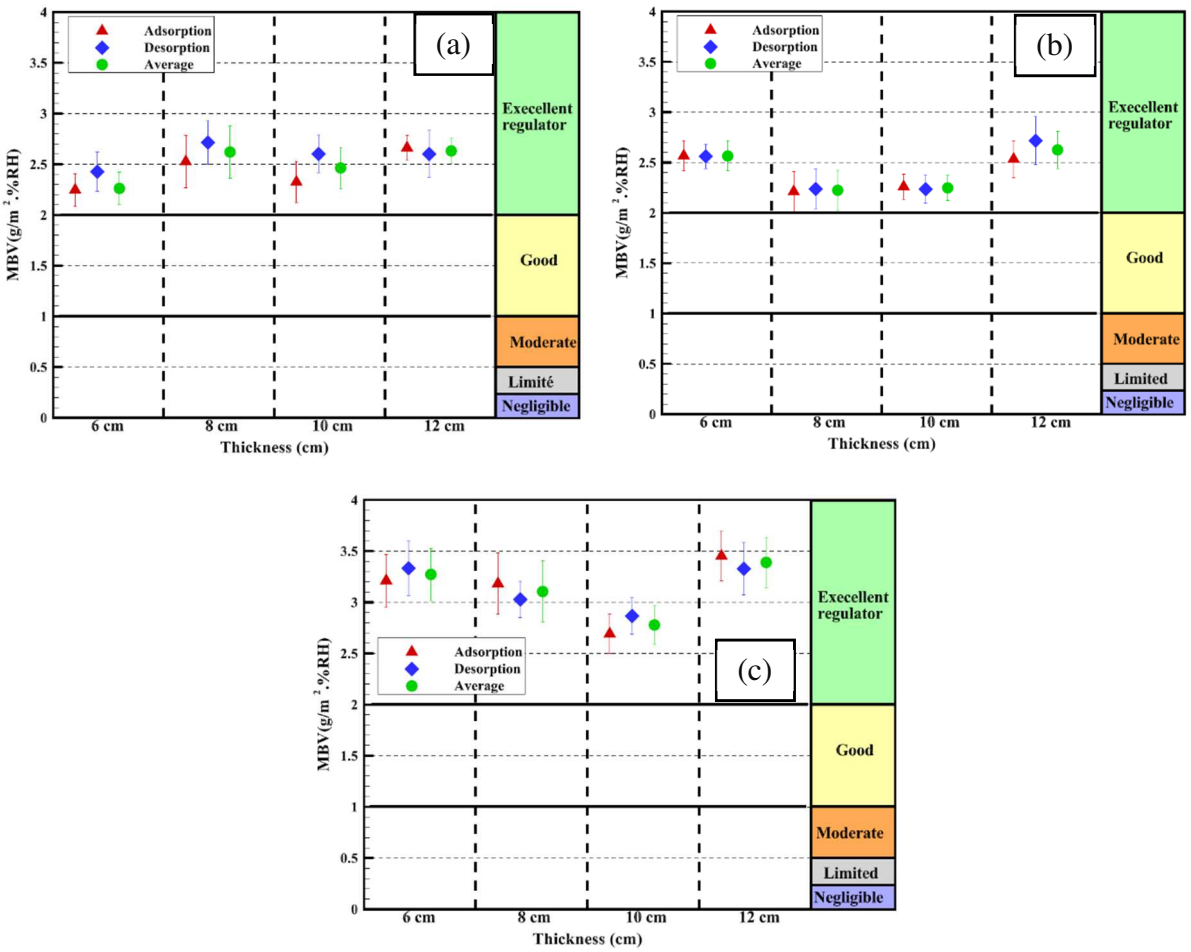


**Fig. 14**. Moisture buffer values for different thickness of the samples (a) LHC (b) LGB and (c) GGB

In Fig. 15, a comparison between the MBV and the density values obtained for the studied biocomposites (with a thickness of 10 cm) and those found in the literature for other composites and other commonly used building materials. The MBV of straw biocomposite is in the same order of magnitude as that of the mentioned biobased materials and it is largely higher than that of conventional building materials as cellular concrete. It is also clear in the fig 15 that the smaller the density, the higher the MBV of the material. However, it should be noted that the most influencing factor on the MBV of the material is the pore distribution and its connectivity.

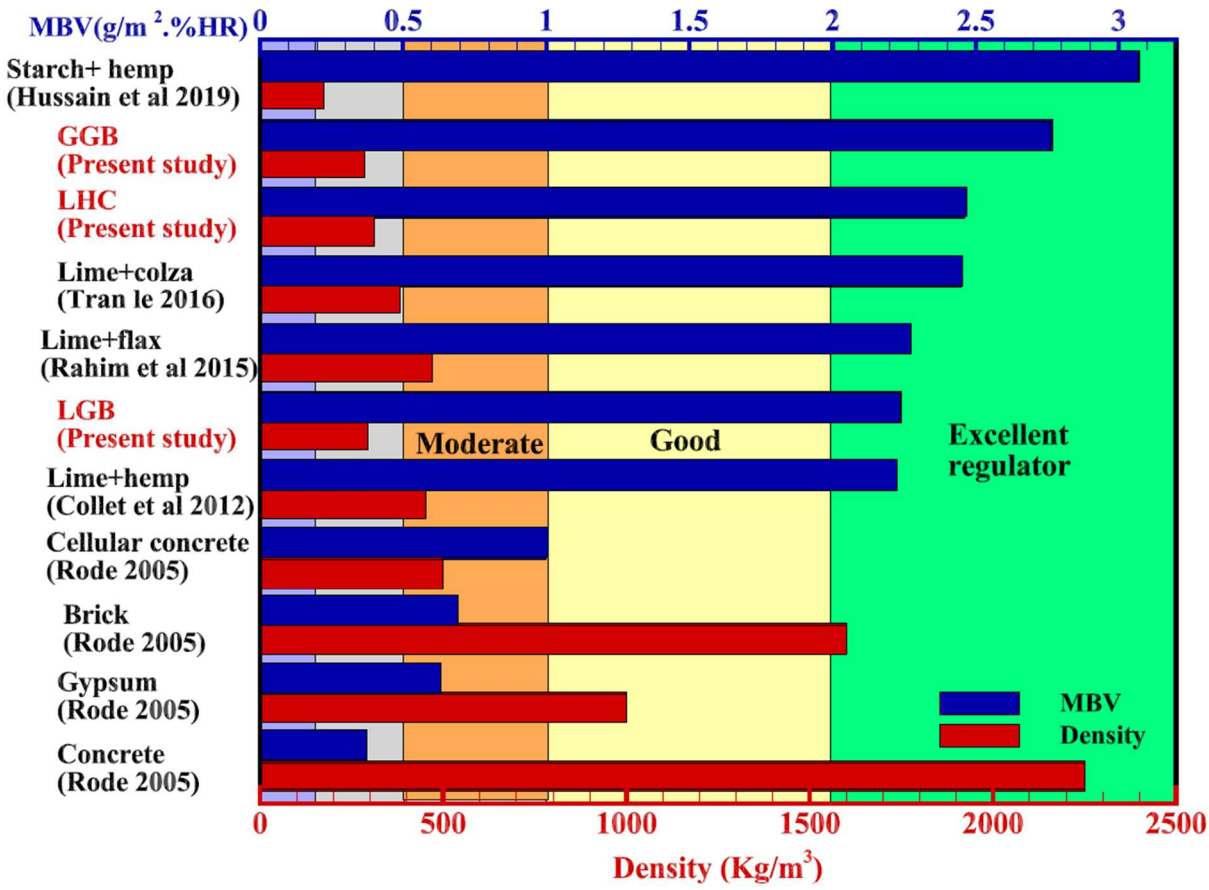


476

477 **Fig. 15**. MBV and density of the studied composites in comparison with other materials in the

478 literature

479 # 4 Conclusion

480

481 The objective of this paper was to study the hygric properties of the three new straw biobased

482 materials with different constituents. The sorption-desorption curves showed a similar pattern

483 to other porous materials studied in the literature such as hemp concrete. A large hysteresis

484 was observed in the case of the lime-based composites, explained by the existence of the ink-

485 bottle shaped pores or the consumption of the water absorbed by the carbonation reaction. The

486 gypsum-based composite has a different behavior than the lime-based composites, which

487 confirms that the type of binder strongly influences the moisture storage of the composite

488 material. All three composites showed high water vapor permeability (low resistance to water

489 vapor diffusion) due to their high open porosity, which allows them to be qualified as highly

hygroscopic materials. In other words, they can contribute to naturally regulate the hygrometry of the interior air of the buildings. The coupling of the results of sorption-desorption and those of the permeability to the water vapor have allowed to deduce the isothermal water vapour diffusivity of the materials. Finally, the moisture buffer value of three composites is measured as a function of the thickness of the materials. The values found made it possible to classify the three composites as excellent moisture regulators without any effect of the thickness as the thicknesses tested were all greater than the penetration depth. The results obtained showed the good hygric performance (permeable to water vapor and moisture regulator) of the studied materials compared to the other classical materials often used in the construction sector.

# 5 Acknowledgements

The authors gratefully acknowledge the ‘‘REGION CENTRE” for the financial support of the research program PEPITE.

# 6 References

[1] C. Ingrao, A. Lo Giudice, J. Bacenetti, C. Tricase, G. Dotelli, M. Fiala, V. Siracusa, C. Mbohwa, Energy and environmental assessment of industrial hemp for building applications: A review, Renew. Sustain. Energy Rev. 51 (2015) 29–42. https://doi.org/10.1016/j.rser.2015.06.002.

[2] T. Jami, S.R. Karade, L.P. Singh, A review of the properties of hemp concrete for green building applications, J. Clean. Prod. 239 (2019) 117852. https://doi.org/10.1016/j.jclepro.2019.117852.

[3] M.P. Sáez-Pérez, M. Brümmer, J.A. Durán-Suárez, A review of the factors affecting the properties and performance of hemp aggregate concretes, J. Build. Eng. 31 (2020). https://doi.org/10.1016/j.jobe.2020.101323.

[4] F. Benmahiddine, F. Bennai, R. Cherif, R. Belarbi, A. Tahakourt, K. Abahri, Experimental investigation on the influence of immersion/drying cycles on the hygrothermal and mechanical properties of hemp concrete, J. Build. Eng. 32 (2020) 101758. https://doi.org/10.1016/j.jobe.2020.101758.

[5] A. Laborel-Préneron, C. Magniont, J.E. Aubert, Hygrothermal properties of unfired earth bricks: Effect of barley straw, hemp shiv and corn cob addition, Energy Build.

178 (2018) 265–278. https://doi.org/10.1016/j.enbuild.2018.08.021.

[6] B. Seng, C. Magniont, S. Lorente, Characterization of a precast hemp concrete block. Part II: Hygric properties, J. Build. Eng. 24 (2019) 100579. https://doi.org/10.1016/j.jobe.2018.09.007.

[7] K.Sing, Reporting physisorption data for gas/solid systems with special reference to the determination of surface area and porosity (Recommendations 1984). Pure and Applied Chemistry. 1985;57(4): 603-619. https://doi.org/10.1351/pac198557040603.

[8] D. Samri, Analyse physique et caractérisation hygrothermique des matériaux de construction: approche expérimentale et modélisation numérique, PhD thesis INSA de Lyon 2008.

[9] A. Bouguerra, H. Sallée, F. De Barquin, R.M. Dheilly, M. Quéneudec, Isothermal moisture properties of wood-cementitious composites, Cem. Concr. Res. 29 (1999) 339–347. https://doi.org/10.1016/S0008-8846(98)00232-4.

[10] E. Latif, M. Lawrence, A. Shea, P. Walker, Moisture buffer potential of experimental wall assemblies incorporating formulated hemp-lime, Build. Environ. 93 (2015) 199–209. https://doi.org/10.1016/j.buildenv.2015.07.011.

[11] F. Bennai. Étude des mécanismes de transferts couplés de chaleur et d'humidité dans les matériaux poreux de construction en régime insaturé. PhD thesis, Université de La Rochelle, 2017.

[12] B. Mazhoud. Elaboration et caractérisation mécanique, hygrique et thermique de composites bio-sourcés. PhD thesis, INSA de Rennes, 2017.

[13] J. Chamoin. Optimisation des propriétés (physiques, mécaniques et hydriques) de bétons de chanvre par la maîtrise de la formulation. PhD thesis, INSA de Rennes, 2013.

[14] N. Belayachi, D. Hoxha, I. Redikutseva, Etude comparative du comportement hygrothermique des matériaux à base de fibres végétales, 33ème Rencontres de l'AUGC. (2015) 1–8.

[15] Y. Brouard, N. Belayachi, D. Hoxha, N. Ranganathan, S. Méo, Mechanical and hygrothermal behavior of clay – Sunflower (Helianthus annuus) and rape straw (Brassica napus) plaster bio-composites for building insulation, Constr. Build. Mater. 161 (2018) 196–207. https://doi.org/10.1016/j.conbuildmat.2017.11.140.

[16] F. Collet, J. Chamoin, S. Pretot, C. Lanos, Comparison of the hygric behaviour of three hemp concretes, Energy Build. 62 (2013) 294–303. https://doi.org/10.1016/j.enbuild.2013.03.010.

[17] ISO 12572:2016 Hygrothermal performance of building materials and products-Determination of water vapour transmission properties -Cup method

[18] F.Collet. Caractérisation hydrique et thermique de matériaux de génie civil à faibles impacts environnementaux. PhD thesis, INSA Rennes, 2004.

[19] A. Evrard. Transient hygrothermal behavior of Lime-Hemp Materials. PhD thesis, Universite Catholique De Louvain , 2008.

[20] R. Walker and S. Pavia. Impact of hydration on the properties of hemp lime concrete. Civil engineering research in Ireland CERAI, Belfast, 2014.

563 [21] M. Rahim, O. Douzane, A.D. Tran Le, G. Promis, B. Laidoudi, A. Crigny, B. Dupre, T.
564 Langlet, Characterization of flax lime and hemp lime concretes: Hygric properties and
565 moisture buffer capacity, Energy Build. 88 (2015) 91–99.
566 https://doi.org/10.1016/j.enbuild.2014.11.043.

567 [22] M. Rahim, O. Douzane, A.D. Tran Le, G. Promis, T. Langlet, Characterization and
568 comparison of hygric properties of rape straw concrete and hemp concrete, Constr.
569 Build. Mater. 102 (2016) 679–687. https://doi.org/10.1016/j.conbuildmat.2015.11.021.

570 [23] M.K.Kumaran, J. Lackey, N. Normandin, D. Van Reenen, & F.Tariku, (2002).
571 Summary report from task 3 of MEWS project at the Institute for Research in
572 Construction-Hygrothermal properties of several building materials. Research Repor-
573 IRC-RR-110. Institute for Research in Construction, National Research Council
574 Canada, 2002, p. 73

575 [24] F. Collet, S. Pretot, Experimental investigation of moisture buffering capacity of
576 sprayed hemp concrete, Constr. Build. Mater. 36 (2012) 58–65.
577 https://doi.org/10.1016/j.conbuildmat.2012.04.139.

578 [25] C. Rode et al, Moisture buffering of building materials. Technical University of
579 Denmark, Department of Civil Engineering, 2005.

580 [26] S. Dubois, A. Evrard, and F. Lebeau. Hygrothermal modelling of lime-hemp concrete
581 used as building material and indoor climate buffering characterization. 2012.

582 [27] A. Piot, T. Béjat, A. Jay, L. Bessette, E. Wurtz, L. Barnes-Davin, Study of a hempcrete
583 wall exposed to outdoor climate: Effects of the coating, Constr. Build. Mater. 139
584 (2017) 540–550. https://doi.org/10.1016/j.conbuildmat.2016.12.143.

585 [28] Y. Jiang, A. Phelipot-Mardele, F. Collet, C. Lanos, M. Lemke, M. Ansell, A. Hussain,
586 M. Lawrence, Moisture buffer, fire resistance and insulation potential of novel bio-clay
587 plaster, Constr. Build. Mater. 244 (2020) 118353.
588 https://doi.org/10.1016/j.conbuildmat.2020.118353.

589 [29] A. Hussain, J. Calabria-Holley, M. Lawrence, M.P. Ansell, Y. Jiang, D. Schorr, P.
590 Blanchet, Development of novel building composites based on hemp and multi-
591 functional silica matrix, Compos. Part B Eng. 156 (2019) 266–273.
592 https://doi.org/10.1016/j.compositesb.2018.08.093.

593 [30] B. Ismail, N. Belayachi, D. Hoxha, Optimizing performance of insulation materials
594 based on wheat straw, lime and gypsum plaster composites using natural additives,
595 Constr. Build. Mater. 254 (2020). https://doi.org/10.1016/j.conbuildmat.2020.118959.

596 [31] I. Langmuir. The adsorption of gases on plane surfaces of glass, mica and platinum.
597 Journal of the American Chemical society, 40(9) :1361–1403, 1918.

598 [32] S. Brunauer, PH. Emmett, and E. Teller. Adsorption of gases in multimolecular layers.
599 Journal of the American chemical society, 60(2) :309–319, 1938.

600 [33] V. Cérézo. Propriétés mécaniques, thermiques et acoustiques d'un matériau à base de
601 particules végétales : approche expérimentale et modélisation théorique. PhD thesis,
602 Institut National des Sciences Appliquées de Lyon, 2005.

603 [34] F. Collet, S. Prétot, C. Lanos, Hemp-Straw Composites: Thermal and Hygric
604 Performances, Energy Procedia. 139 (2017) 294–300.
605 https://doi.org/10.1016/j.egypro.2017.11.211.

606 [35] Réglementation thermique: Règles Th-U-Fascicule 2 (2005).

607 [36] DA. De Vries. Simultaneous transfer of heat and moisture in porous media. Eos,
608 Transactions American Geophysical Union, 39(5) :909–916, 1958.

609 [37] J. Arfvidsson. A new algorithm to calculate the isothermal moisture penetration for
610 periodically varying relative humidity at the boundary. Nordic Journal of Building
611 Physics, 2, 1999.

612